Observation of a Heterogeneous Source of OClO from the Reaction of ClO Radicals on Ice

J. R. McKeachie

Department of Chemistry, 516 Rowland Hall, University of California, Irvine, California 92697-2025

M. F. Appel

Department of Biology, Chemistry and Environmental Science, Christopher Newport University, 1 University Place, Newport News, Virginia 23606

U. Kirchner

Ford Forschungszentrum Aachen GmbH, Süsterfeldstrasse 200, D-52072 Aachen, Germany

R. N. Schindler

Christian-Albrechts Universität zu Kiel, Institut für Physikalische Chemie, Ludewig-Meyn-Strasse 8, 24098 Kiel, Germany

Th. Benter*

Bergische Universität Wuppertal, FB C—Mathematik und Naturwissenschaften, Gauss Strasse 20, 42097 Wuppertal, Germany

Received: February 15, 2004; In Final Form: June 8, 2004

Experiments presented in this contribution demonstrate a heterogeneous source of several chlorine oxides, in particular OClO and $ClClO_2$, from ClO radicals passed over water−ice surfaces at low pressures. ClO radicals were generated in a flow system and reaction products were monitored by UV−vis absorption spectroscopy and time-of-flight mass spectrometry using electron-impact and resonance-enhanced multiphoton ionization, respectively. In all experiments an efficient release of OClO into the gas phase was observed *upon ice evaporation*. No such gas-phase products directly formed in the initial interaction of ClO with the ice surface were detected. To explain these findings, it is proposed that a $ClO{\cdot}H_2O$ complex is formed in a rapidly established equilibrium between ClO monomers and gas-phase H_2O. The existence of this complex as well as a surface-enhanced ClO-recombination process is assumed to be responsible for the observed efficient reactive uptake of ClO radicals onto the ice surface. Several possible reaction pathways resulting in the formation of the experimentally observed products are presented. As an alternative pathway, H_2O-facilitated gas phase disproportionation of ClO yielding hypochlorous and chlorous acid and subsequent deposition on the surface is considered. The observation of OClO evolving from an ice surface previously exposed to ClO radicals, as well as the lack of any symmetric ClOOCl dimer formation in the presence of high water mixing ratios, carries some possible atmospheric implications: First, there is currently a missing source of OClO in the chemically perturbed polar vortex. The ClO + BrO reaction is presently believed to be the only source of OClO in the stratosphere, although several studies show this reaction system to severely underestimate OClO production in this atmospheric subsystem. It is suggested that this experimentally observed heterogeneous source of OClO could carry implications for the total atmospheric OClO budget. Second, the $ClO{\cdot}H_2O$ complex could directly or indirectly affect the ClOOCl formation rate and thus strongly impact homogeneous chlorine chemistry.

Introduction

Highlighted by the work of Molina and Rowland in 1974,[1] the chemistry of the stratospheric ozone layer has been a major focus of atmospheric research for nearly 30 years. Studies in this area have discovered several free-radical chain reactions that catalyze ozone destruction, for example, ClO_x, BrO_x, and HO_x cycles, and have spurred interest in many trace species involving bromine and chlorine.[2,3] The discovery of the almost complete disappearance of stratospheric ozone over Antarctica during winter months by Farman et al.[4] initiated a thorough investigation into the local conditions and the chain of events causing this ozone "hole". Again, much emphasis was placed on the trace species containing chlorine and bromine, including ClO and BrO, products of direct halogen atom reactions with ozone (reactions 1 and 2)

$$Cl + O_3 \rightarrow ClO + O_2 \quad (1)$$

$$Br + O_3 \rightarrow BrO + O_2 \quad (2)$$

* To whom correspondence should be addressed. Fax: +49 (0)241 439 2505. E-mail: tbenter@uni-wuppertal.de.

10.1021/jp049314p CCC: $27.50
Published on Web 10/02/2004

When considering ozone depletion, homogeneous gas phase reactions of ClO and BrO appear to be of most concern. The ClO dimerization cycle (reactions 1, 3, and 4) is thought to be responsible for approximately 70% of the total ozone loss in the polar vortex.[5]

$$ClO + ClO + M \rightarrow ClOOCl + M \quad (3)$$

$$ClOOCl + h\nu \rightarrow 2Cl + O_2 \quad (4)$$

Further, the cross reaction of ClO and BrO (reactions 5a−c) is thought to account for another 25% of the ozone destruction in the Antarctic vortex; besides its contribution to ozone depletion, reaction 5a is heretofore considered the only source of OClO in the stratosphere.

$$BrO + ClO \rightarrow OClO + Br \quad (5a)$$

$$\rightarrow Cl + Br + O_2 \quad (5b)$$

$$\rightarrow BrCl + O_2 \quad (5c)$$

In contrast to the termolecular step 3, reaction 6a, one of the three homogeneous bimolecular components of ClO self-reaction,[6−8] is considered too slow at stratospheric temperatures to produce OClO in significant quantities, and thus is neglected:

$$ClO + ClO \rightarrow OClO + Cl \quad (6a)$$

$$\rightarrow Cl + ClOO \quad (6b)$$

$$\rightarrow Cl_2 + O_2 \quad (6c)$$

Observations from periods of low ozone concentration have revealed OClO to be an indicator of chlorine activation from reservoir species,[9] such as HCl and $ClONO_2$. Upon polar sunrise, molecular chlorine produced in heterogeneous nighttime reactions of chlorine reservoir species on ice particulates undergoes photolysis, initiating catalytic ozone depletion cycles.[10] The BrO and ClO formed in ozone destruction cycles react to form OClO via reaction 5a, and the amount of OClO measured signifies the production of ClO and BrO. In fact, the OClO abundance is used to calculate mixing ratios for ClO and BrO.[11] Production of OClO, then, gives a qualitative and quantitative measure of chlorine activation during polar winter.

Along with measurements of the conditions concerning the ozone hole, computer models are also used to investigate this phenomenon. Very successful results have been produced that model the ozone hole itself and profiles of the important species involved.[10,12] However, Fish and Burton[13] report that the loss of ozone can be modeled only with a ±25% accuracy, and they go on to say that the uncertainty in the ClO/BrO reaction system is responsible for 21% of the error in modeled ozone loss. Other studies have reported significant discrepancies in the modeled and measured concentrations of OClO; in these studies, present models are continually predicting lower OClO concentrations during chlorine activation than measured abundances.[14] Furthermore, studies have included other observations during this time involving ClO and OClO that cannot be modeled satisfactorily using known chemistry.[15,16] Thus, it is clear there is some contribution to these observations of the chemically perturbed polar vortex chemistry from some hitherto unreported phenomena or reactions.

Investigations carried out by Molina et al.[17] intimated that another source of OClO could be afforded in a process involving a reaction of ClO radicals in the presence of humidity. Further research by Kirchner et al.[18] and others[19,20] showed OClO evolving from an *evaporating* ice surface after ClO radicals were passed over it, as well as other chlorine oxides not expected to be present. In the present paper, subsequent investigations based on the work of Kirchner et al.[18] and Kirchner[20] are discussed. Past and present results are compared in an effort to determine a reaction pathway for the generation of these chlorine oxides, with a focus on possible heterogeneous processes taking place on or in the ice surface. Additionally, a qualitative investigation into the efficiency of these processes is presented in an attempt to establish that they could represent a significant source of OClO in the stratosphere as well as in other areas of the atmospheric system, for example, the arctic troposphere.

Experimental Section

Monitoring Techniques. Experiments were monitored using UV−vis absorption spectroscopy and either electron impact (EI) or resonance-enhanced multiphoton time-of-flight mass spectrometry (REMPI TOF MS) as schematically shown in Figure 1. The UV−vis absorption section of the flow system consisted of a 50 × 7 cm circular-jacketed quartz absorption cell equipped with White cell optics, yielding a total path length of 200 cm. The cell was irradiated with a Hamamatsu L 636 Deuterium discharge lamp. Using fiber optics, both the transmitted and the incident light were concomitantly coupled to a Jobin-Yvon HR 250 spectrograph supplied with a double diode array detector. The two arrays of the detector consisted of 512 pixels each. In most experiments a 300 lines/inch grating was used, leading to a spectral detection range of 170 nm. The absorption spectra were processed with the commercial Parallel Optical Simultaneous Multichannel Analysis (POSMA) software package.

A Bruker TOF1 reflectron time-of-flight mass spectrometer was used to simultaneously monitor ion signals of interest in the range $30 < m/z < 300$. A homemade valve allowed pulsed molecular beam sampling of the flow, see inset b) in Figure 1. Using EI, complete mass spectra were recorded and co-added with repetition rates up to 500 Hz. The electron source was arranged perpendicularly to both the laser and molecular beam orientation, as shown in the inset a) of Figure 1. EI-TOF MS was employed to monitor parent ions of OClO, Cl_2, Cl_2O_2, and Cl_2O_3, see results section for further details. The laser ionization source consisted of a Lambda Physik excimer pumped frequency doubled dye laser system. This setup has been described elsewhere.[21−23] With this technique ClO radicals and Cl_2O were unambiguously monitored in the complex reaction mixtures, see results section. Using a variety of experimental arrangements, the flow of ClO radicals was directed onto dry glass or ice surfaces. Figure 2 shows schematic diagrams of the four different experimental designs employed.

Chemical Sources of Reactants Used. In the course of these experiments, several in-situ sources for chlorine oxides were employed. OClO, Cl_2O, and $ClClO_2$ were prepared using their respective standard laboratory generation procedures.[24−27] In all cases the effluent was monitored by UV−vis and EI MS to corroborate correct reactant formation.

Chlorine oxide radicals were prepared from a number of sources based on atom initiated abstraction reactions. These sources generated ClO radicals in either OClO-free, O_3-free, or nearly Cl_2-free gas flows. The very efficient reaction between chlorine atoms and ozone (1) generates up to 1×10^{13} ClO radicals/cm^3 in the flow reactor:

$$Cl + O_3 \rightarrow ClO + O_2 \quad (1)$$

This source operated free from higher chlorine oxides (see below) at the expense of either significantly high remaining [O_3]

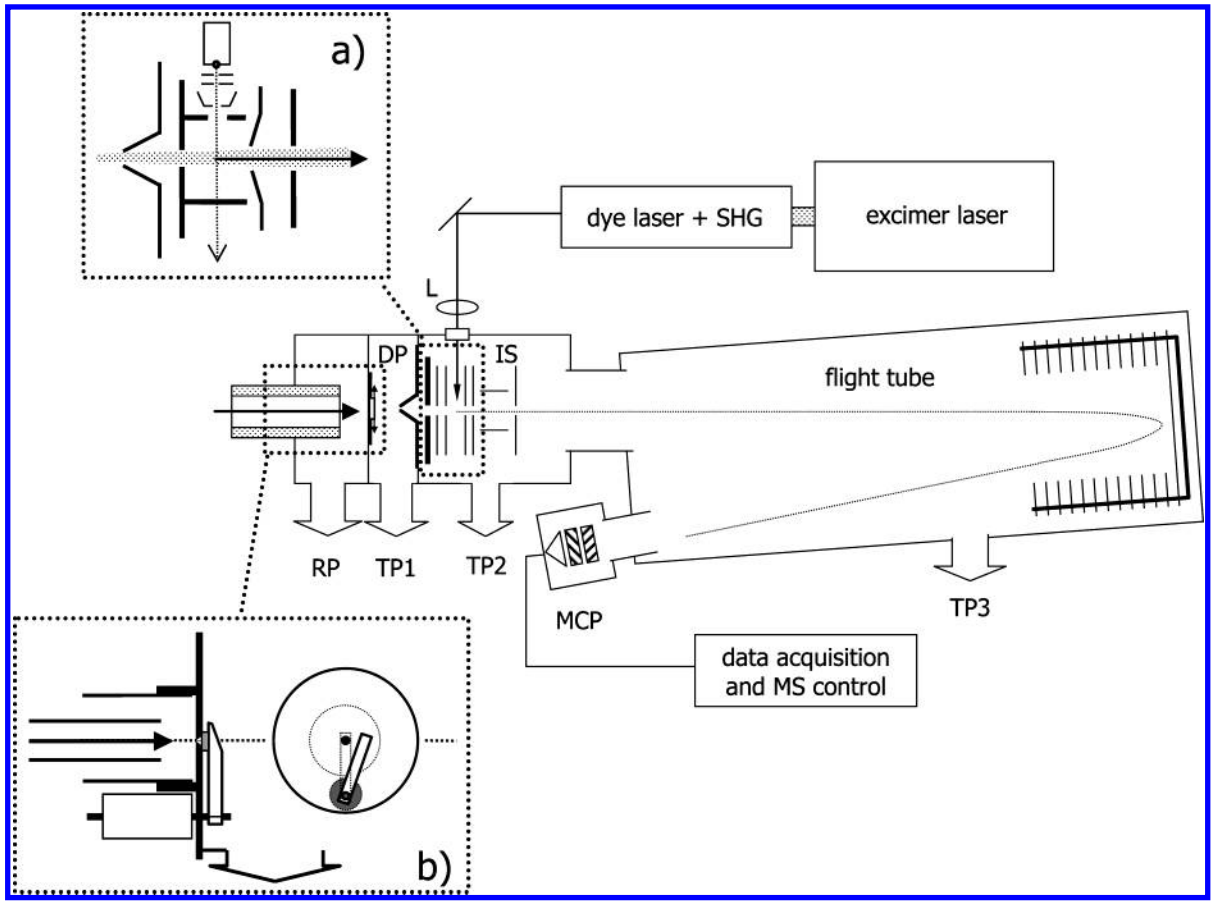

Figure 1. Mass-spectrometric detection system consisting of a temperature-controlled pulsed inlet stage, differential pumping system (DP), combined laser/electron impact ionization source (IS), reflectron time-of-flight mass analyzer, and data-acquisition/control system. The timing of the lasers, electron source, inlet valve, and mass spectrometer is computer controlled. (Inset a) Schematic diagram of the pulsed electron source arranged perpendicularly to the laser and molecular beam, respectively. The electron beam is pulsed with a repetition rate of up to 500 Hz, the pulse width ranges from 0.25 to 20 μs. (Inset b) Schematic diagram of the pulsed inlet valve. Valve opening times are adjustable from 100 μs to continuous operation, depending on the inlet system pressure, which can range from 0.5 to 100 mbar. The nozzle orifice is opened by the solenoid-driven turning lever. The Teflon tip of the lever reduces friction and seals the orifice in the closed position. RP = rough pump, TP = turbo molecular pump, L = lens, SHG = second harmonic generation stage of the dye laser, MCP = multichannel plates.

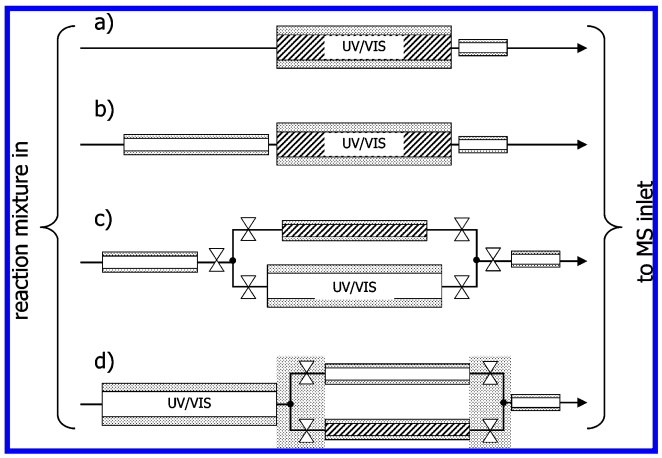

Figure 2. Temperature-controlled chemical reactors used during the course of the experiments. Grey, shaded areas indicate actively cooled regions. Hatched areas indicate ice-covered surfaces, see the Experimental section for details. The valve setup in (c) is realized with two three-way valves in an all-closed position. The valves in (d) are electronically controlled. UV/Vis = UV−vis absorption cell equipped with white optics and double diode array detector.

or $[Cl_2]$. The latter reached several 10^{14} molecules/cm^3 when ozone was titrated below the UV−vis-detection limit of 10^{12} molecules/cm^3.

Because of the convenience of this system, the majority of the experiments described here were conducted with the Cl + O_3 source as follows: ozone and chlorine were added to the carrier gas flow at typical concentrations of $\approx 10^{14}$ molecules/cm^3. The microwave discharge was then ignited and the final flow rates of the ozone, chlorine, and diluting helium were adjusted so that a UV−vis ClO absorption spectrum as shown in the inset in Figure 3 was attained, with no OClO detectable by either absorption or mass spectrometric signals. As discussed above, the gas flow typically contained excess Cl_2, identified by its continuous absorption with a maximum at 330 nm and EI mass signals at m/z = 70, 72, and 74. Under these conditions, approximately 5×10^{12} ClO radicals/cm^3 were generated, as determined by gas titration with NO, shown in Figure 3. In all runs, ozone was nearly quantitatively consumed shortly after ignition of the discharge. Unequivocal identification of thermalized ClO radicals was possible by employing mass selective REMPI detection at parent ion mass m/z = 51. See Results section for further details.

The reaction sequence 7a−c

$$OClO + O \rightarrow ClO + O_2 \quad (7a)$$

$$ClO + O \rightarrow Cl + O_2 \quad (7b)$$

$$Cl + OClO \rightarrow 2\,ClO \quad (7c)$$

generated ClO radicals in high yields and, more importantly

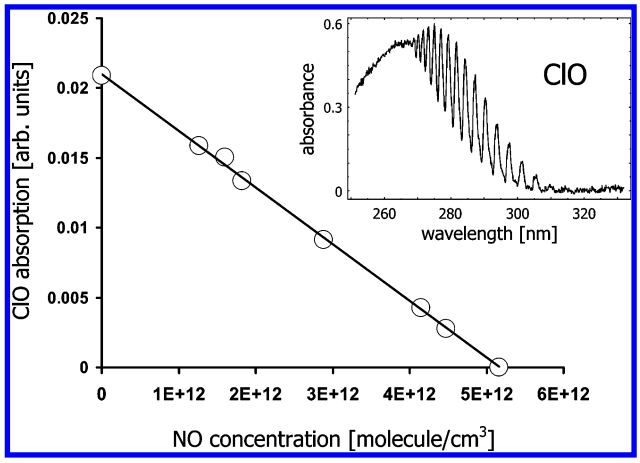

Figure 3. UV−Vis absorption calibration run for ClO radicals employing titration with NO. The inset shows an uncorrected UV−vis absorption spectrum typically obtained using the OClO + O or O_3 + Cl radical source, see the Experimental section for details. $T = 298$ K, $p = 2.4$ mbar.

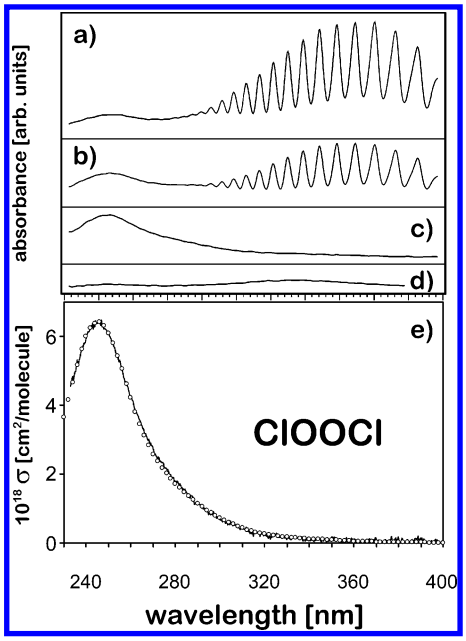

Figure 4. Panels (a)−(d): Sequence of raw UV−vis absorption spectra recorded in the wavelength range 230 nm < λ < 400 nm using the OClO + O radical source for preparation of ClOOCl. From (a) to (d) the O-atom concentration is increased stepwise. $[OClO]_{initial} = 5 \times 10^{14}$ molecules/cm^3, T = 223 K, $p = 25$ mbar. Panel (a) shows the OClO absorption while [O] = 0, panels (b) and (c) show the appearance of ClOOCl and disappearance of OClO respectively, and panel (d) shows the resultant Cl_2 spectrum after addition of excess O atoms. The lower panel (e) shows a vertically expanded and Cl_2-corrected spectrum of ClOOCl obtained in this work (solid line) normalized to a reference spectrum from DeMore et al.[29] (circles). Excellent agreement is found throughout the spectral region monitored.

for some of the present experiments, completely free of ozone. The oxygen atom concentration was adjusted such that no OClO was detectable in the effluent. Although this system was easy to handle, in all experiments concerning heterogeneous OClO formation both sources, Cl + O_3 and OClO + O, were used to confirm the data obtained.

Cl, O, and F atoms were generated by passing the respective diluted molecular gases though a microwave discharge. The dissociation rates depended on the carrier gas flow velocity and tube pressure, and were generally on the order of ≤8%, ≤25%, and >85%, respectively. It is unclear why the Cl atoms recombined rapidly after dissociation. The recombination rate strongly depended on the surface conditions in the discharge region as well as on Cl_2 impurities. Rarely, Cl atoms were generated indirectly via the reaction F + HCl, which takes advantage of the low recombination rate of F atoms in the system. Using this method, Cl atoms were produced with only minor Cl_2 contribution.

O_3 was prepared in a commercial ozone generator using a flow of ultrapure oxygen. The generator effluent was collected on a silica gel trap held at −70 °C with an acetone/dry-ice bath. Ozone was added to the experiment by passing a helium gas stream through the temperature-controlled silica gel trap.

The ultrapure grade gases He, O_2, F_2, Cl_2 (halogens 5% in He), and HCl (10% in He) were obtained from Messer-Griesheim, BCl_3 (>99.9%) was obtained from Merck, and the gases were used without purification. Cl_2 was obtained from Matheson with a stated purity of 98%. $NaClO_2$ powder (>80 wt %, Sigma Aldrich) and yellow Hg(II)oxide (>99 wt %, Merck) were purchased as *pro analysi* grades and used without further treatment.

Ice surfaces were prepared either through spraying a mist onto the inside walls of a precooled flow tube, pumping He gas saturated with water vapor through the cooled tube, or simply by cooling the tube while exposed to laboratory air. All methods took approximately 30 min to complete. It is pointed out that the ice-surface generation procedure had *no effect* on the observed results.

Results

Experiments with ClO Exposure to Dry Glass Surfaces. *UV−Vis Spectroscopic Data.* The experimental results described in this section were all performed in absence of any *visible* ice film or frost in the flow tube. "Dry" thus means that no water-containing gas stream or gaseous water was flown or sprayed onto the precooled glass surfaces (see next section). Figure 4 displays a typical series of UV−vis spectra obtained using setup B with a dry flow tube surface and the OClO + O radical source for ClO preparation. Starting with $[OClO] = 5 \times 10^{14}$ molecules/cm^3, addition of increasing amounts of O-atoms lead to the expected decrease in OClO absorption and simultaneous buildup of ClOOCl (traces a and b). Under the slow flow conditions applied, that is, 1.2 m/s flow velocity at 25 mbar total pressure, $T = 223$ K, nearly quantitative formation of the symmetric ClO dimer is observed (trace c). These results are in good agreement with model calculations using the LARKIN software package.[20,28] Addition of excess O atoms lead to a strong increase in the Cl_2 absorption, as seen in trace d. Trace e shows a Cl_2-corrected UV−vis spectrum of the reactor effluent normalized to the currently recommended data for ClOOCl from DeMore et al.,[29] shown as circles. Excellent agreement is found throughout the spectral region recorded and it is a reasonable assumption that the symmetric dimer is the major ClO recombination product under the stated experimental conditions. Mass-spectrometric data further strengthen these findings (see below). In one single experiment, all products generated in the OClO + O system were trapped at 77 K under slow flow conditions and $p = 30$ mbar using setup A. Figure 5 shows the fractionated release upon gradually warming the absorption cell to room temperature. The O_3 and Cl_2 are released first as expected (not shown), followed by ClOOCl and finally Cl_2O_3. Note that no $ClClO_2$ was observed in this run.

Mass Spectrometric Data. In Figure 6 are plotted normalized 70 eV electron impact reference mass spectra for the chlorine

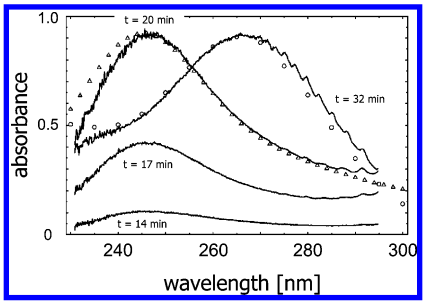

Figure 5. UV−Vis absorption spectra recorded consecutively at the indicated times upon gradual warming of the trapped cell content from 77 K to room temperature, see the Results section for details. First O_3 and Cl_2 are released (not shown), then ClOOCl, and finally Cl_2O_3. For the latter two chlorine oxides reference data are included. Triangles: ClOOCl, from DeMore et al.,[29] circles: Cl_2O_3, from Wayne et al.[80]).

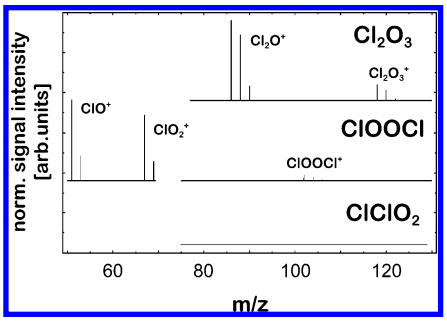

Figure 6. 70-eV electron impact mass spectra recorded under different conditions for Cl_2O_3 (top), ClOOCl (middle), and $ClClO_2$ (bottom) as discussed in the Experimental section. Due to interfering background signals individual regions in the mass spectra are blanked out (m/z < 78 for Cl_2O_3, 70 < m/z < 75 for ClOOCl, and m/z < 75 for $ClClO_2$). Note that ClOOCl is unequivocally identified in mixtures with $ClClO_2$ and Cl_2O_3 present upon monitoring the parent peak at m/z = 102 ($^{35}ClOO^{35}Cl$).

oxides Cl_2O_2, Cl_2O_3, and $ClClO_2$, recorded under different conditions. The Cl_2O_3 mass spectrum was recorded during the warm-up phase of a ClO-experiment conducted at liquid nitrogen temperatures, cf. Figure 5. In this run the OClO + O system was employed for ClO radical generation, but in contrast to all other experiments, OClO was kept in excess. $ClClO_2$ mass spectral data were obtained by an in situ preparation using the reaction $FClO_2 + BCl_3$.[27] The symmetric ClOOCl data are from the 233 K run shown in Figure 4c. The absence of electron impact mass signals at m/z = 118 ($^{35}Cl_2O_3^+$) and m/z = 86 ($^{35}Cl_2O^+$) in this and similar runs leads to the conclusion that the symmetric dimer is by far the dominating species formed in the reaction system under dry conditions.

Surprisingly, employing REMPI MS, measurable quantities of Cl_2O were detected as a product of the ClO recombination reaction in the absence of a previously prepared ice surface in the gas flow. It is pointed out, however, that some surface water was always present on the cold flow tube walls, since the in situ sources for the chlorine oxides, as discussed in the Experimental Section, required the addition of water droplets to the solid reactant mixture. Upon flowing the reaction gases, a fraction of this water was transported to the reactor region and condensed on the cold walls.[19] Electron impact ionization of Cl_2O is discovered to be two to three orders of magnitude less sensitive than REMPI. Thus, the formation of Cl_2O in this reaction system was not previously observed. The Cl_2O formation was independent of the dynamic source used for ClO radical preparation, and there is currently no literature available that describes the formation of gas-phase Cl_2O in either the OClO + O or O_3 + Cl reaction system. The Cl_2O concentration was found to be roughly a factor of 50 to 100 lower than [ClOOCl]. Due to the much higher sensitivity of REMPI toward nascent ClO radical detection as compared to UV−vis, a residual ClO concentration of 3×10^{11} molecule/cm^3 was also quantified in the flow tube effluent. This is in full agreement with LARKIN model calculations.[28]

When using REMPI detection of photolabile species, photolytic processes occurring at intermediate levels in the multiphoton ionization pathway can render the interpretation of the acquired mass spectra difficult. It is pointed out that in the present study, REMPI allowed for unambiguous determination of the origin of the signals recorded at m/z = 51 (ClO^+) when scanning the wavelength range from λ = 336 nm to 345 nm, as discussed in the following paragraphs.

In the present experiments ClO^+ signals can potentially arise from either thermalized ClO radicals (reaction 8), or photolytic (reaction 9) and/or ionic fragmentation (reactions 10a and b) of precursors:

$$ClO + (2 + 1)\, h\nu \rightarrow ClO^+ \quad (8)$$

$$OClO + h\nu \rightarrow ClO + O, \text{ followed by (8)} \quad (9)$$

$$Cl_2O + (2 + 1)\, h\nu \rightarrow Cl_2O^+ \quad (10a)$$

$$Cl_2O^+ + nh\nu \rightarrow ClO^+ + Cl\ (n = 1, 2, ...) \quad (10b)$$

Each route leads to a unique REMPI spectrum:[30] The direct resonant pathway (reaction 8) generates the ion from the molecular ground state and reflects a rovibrational population corresponding to the experimental conditions, that is, in the present case of T = 233 K. Photolysis of a precursor molecule (reaction 9) generally produces rovibrationally and/or electronically excited neutral fragments, which are subsequently ionized. A nonthermal distribution in a REMPI spectrum is a clear indication of the photolytic origin of the ion signals. Ionic fragmentation (reactions 10a and b) is easily determined by monitoring all major fragment ion signals and the parent mass. If all ion signals show identical spectral patterns, ionic fragmentation is most likely the origin of the monitored signal. Most importantly, the spectral response of a primary photolysis product differs from the thermalized neutral precursor. Fortunately, in the present experiments such an unambiguous assignment was possible.

Figure 7 illustrates these general observations. All spectra were generated recording mass m/z = 51 ($^{35}ClO^+$) as a function of wavelength. The top trace shows the REMPI spectrum of thermalized ClO radicals (T = 233 K) generated in a two-photon resonant, three-photon ionization process via the C $^2\Sigma^-$ (ν = 0) Rydberg manifold.[31,32] Trace b was recorded at T = 298 K with 5×10^{12} molecules/cm^3 OClO present. The rotational temperature of the ClO radicals monitored is clearly much higher compared to trace a, and $T_{rot} \approx$ 800 K can be calculated using a spectral simulation program package.[19,33,34] Similar findings[35,36] were reported earlier using two-photon absorption LIF. In addition, vibrationally excited ground-state ClO radicals up to ν = 5 were detected (not shown here). Trace c shows the response of m/z = 51 (ClO^+) when a flow containing 5×10^{12} molecules/cm^3 Cl_2O was present at T = 298 K. The pattern obtained is completely different from the above spectra and corresponds well to a three-photon transition to the ionization region of Cl_2O and subsequent fragmentation of the parent ion. The appearance potential of ClO^+ from Cl_2O is reported[37] to be 12.3 eV, which is reached upon absorption of a fourth photon. The inset shows the signal pattern recorded in a high-resolution

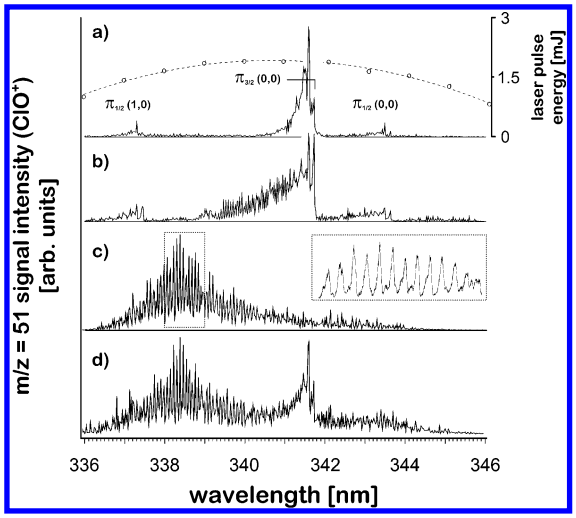

Figure 7. REMPI spectra recorded at $m/z = 51$ (ClO^+) under different conditions. Trace (a): Signal response of thermalized ClO radicals, generated using the OClO + O radical source. OClO is quantitatively consumed, as shown in the inset in Figure 3. $T = 233$ K, $p = 2.5$ mbar. Trace (b): REMPI spectrum obtained with 1.5×10^{14} molecules/cm^3 OClO present in the flow. $T = 240$ K, $p = 5$ mbar. The relative intensities of the two Π components of the C ⟵ X (0,0) two-photon transition as well as the rotational line distribution are used to determine the deviation from the thermal ground state population. Clearly, the detected ClO radicals are highly rotationally excited ($T_{rot} \sim 800$ K, cf. Results section). Trace (c) is recorded with 2.5×10^{13} molecules/cm^3 Cl_2O present in the flow. $T = 240$ K, $p = 10$ mbar. The inset shows a high-resolution scan in the wavelength range 338 nm $< \lambda <$ 339 nm used for unambiguous identification of Cl_2O in complex mixtures. Trace (d) shows the mass signal response at $m/z = 51$ when the reactor effluent of the OClO + O source is analyzed. Experimental conditions correspond to the UV−vis spectrum shown in Figure 4c. Subsequent spectral subtraction of the ClO (trace (a)) and Cl_2O (trace (c)) REMPI spectra from (trace (d)) yields a baseline.

scan from 338 nm $< \lambda <$ 339 nm. This unique pattern was used to identify Cl_2O in complex reaction mixtures. Finally, trace d shows a REMPI spectrum obtained from the cell effluent when ClO radicals were directed through the "dry" flow tube held at 233 K, that is, without a *visible* ice or frost layer present. Clearly, residual thermal ClO radicals and completely unexpected Cl_2O molecules are identified. Cl_2O was not detectable by simultaneous UV−vis measurements because of the strong interfering ClOOCl and Cl_2 absorptions (cf. Figure 4c). Upon spectral subtraction of the Cl_2O^+ signals, a residual spectrum as shown in Figure 7a was observed, indicating that no other species capable of producing ClO^+, in particular OClO, were present.

Experiments with ClO Exposure to Ice Surfaces. The most striking difference when running the experiments using an ice-covered flow tube was the quantitative suppression of any observable gas-phase products from the homogeneous ClO selfreaction. In addition, no other gas-phase product arising from known homogeneous or heterogeneous processes was noticeable. Neither the EI MS nor the UV−vis analysis revealed the presence of any compounds other than the initial reactants in the flow tube effluent. This finding was independent of the ClO radical source employed.

It is pointed out that ClOOCl generated upstream of the ice-coated tube using setup D did not react, nor was it noticeably taken up by the ice surface, as determined with EI MS detection. In this case, warming up the isolated, coated flow tube allowed for the recovery of only trace amounts of Cl_2, close to the detection limit of the MS. However, upon doping the ice surface

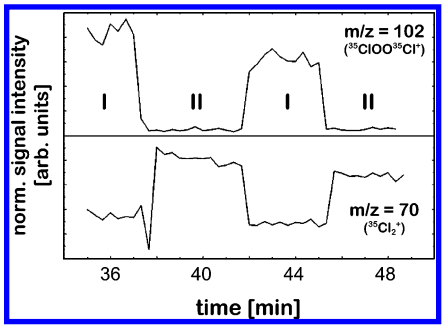

Figure 8. Simultaneously recorded mass signals at $m/z = 102$ ($^{35}ClOO^{35}Cl^+$, top) and $m/z = 70$ ($^{35}Cl_2^+$, bottom), recorded upon switching the reactor effluent repeatedly from the uncoated reference cell of setup D (regions labeled I) to the reaction cell (regions labeled II), which is coated with a 10% HCl ice film. The nonzero background signal at $m/z = 70$ ($^{35}Cl_2^+$) when switching to the reference cell is due to Cl_2, which is always present in varying amounts depending on the ClO radical source used (cf. Figure 4 and Experimental section). Note that ClOOCl reacted quantitatively under the present conditions to yield Cl_2. $T = 213$ K, $p = 25$ mbar.

with HCl, ClOOCl reacted quantitatively and the formation of large amounts of Cl_2 was observed, as shown in Figure 8. Using setup D (cf. Figure 2) the flow containing the ClOOCl dimer was switched repeatedly between the reference cell (regions labeled I in Figure 8) and the covered reaction cell (regions labeled II). As can be seen, mass-spectral data responded accordingly, even after accumulated exposure times of more than 40 min. This result is in full agreement with the report by De Haan and Birks.[38] They measured a fast conversion of ClOOCl on HCl-doped ice surfaces with Cl_2 appearing as the major reaction product.

Any HCl present in the ClO/ice reaction system, either initially or formed in situ, would have been efficiently taken up by the surface.[29] Subsequent reaction of any symmetric dimer present would have lead to Cl_2 formation in the ice, which was not observed. This result corroborates the mass spectrometric and UV−vis absorption findings, and shows clearly that ClOOCl was not formed even in concentrations below the detection limit of these two analytical techniques.

It is concluded that the symmetric dimer formation process is strongly affected by either the presence of an ice surface or by the elevated water vapor concentration in or downstream of the flow tube region (see Discussion). In all experiments described, the water-vapor concentration was only controlled by the temperature of the ice surface, since H_2O was not assumed to be a reactive species in the systems studied.

Upon vaporizing an ice surface that had been exposed to ClO radicals, hitherto unobserved products were released: the asymmetric ClO dimer chloryl chloride, $ClClO_2$, and unexpected large quantities of OClO were clearly identified in UV−vis measurements. The MS measurements confirmed the results obtained with UV−vis, and in addition showed the release of large amounts of HCl upon ice evaporation. Figure 9 shows representative results from these experiments. Frequently, $ClClO_2$ and OClO were observed concomitantly, with $ClClO_2$ having a transient character. In some runs $ClClO_2$ appeared to be a precursor of OClO, particularly after prolonged exposure of the ClO flow to the ice surface. Using very short contact times of <10 s, OClO was the only product observed after warmup. The OClO continued to be released until the ice/water was completely evaporated.

In slow flow experiments using setup C (cf. Figure 2) a quantitative treatment of the total ClO radicals flown over the

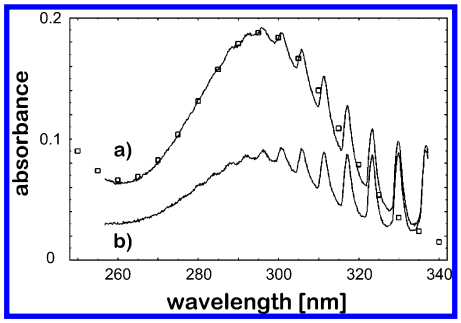

Figure 9. Buildup of the $ClClO_2$ absorption typically observed upon gradually warming up an ice surface that was previously exposed to a flow containing ClO radicals. $T = 230$ K, $p = 2.5$ mbar, $[ClO]_{initial} = 3.5 \times 10^{12}$ molecules/cm^3, integral contact time = 300 s. The absorptions of $ClClO_2$ (and/or OClO) rapidly appear when the ice matrix begins to collapse. Spectrum (a) is recorded 10 s before spectrum (b). The $ClClO_2$ absorption always has a transient character and typically disappears completely in less than 60 s. OClO is quantitatively determined after complete evaporation of the ice. Squares represent $ClClO_2$ reference data from Wayne et al.[80] Using parallel mass spectrometric analysis, no signals at $m/z = 102$ ($^{35}ClOO^{35}Cl^+$) are detected throughout the warmup period.

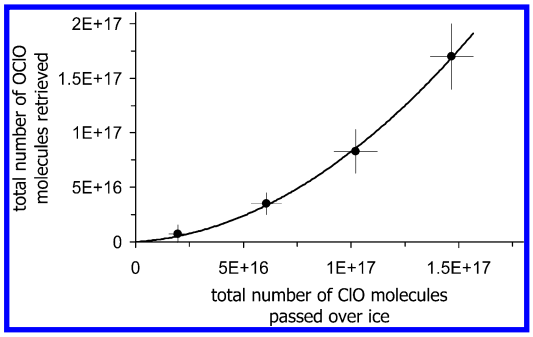

Figure 10. Plot of the calculated total amount of ClO radicals passed over an ice surface of known geometric area vs. the total number of OClO molecules retrieved after warmup, as described in the Discussion section. The total number of ClO radicals passed over the surface is adjusted by variation of the integral contact time of 5 s $< t <$ 60 s. Error bars are given for each individual run. The solid line represents a quadratic regression analysis.

ice surface revealed that up to 100% of the ClO had been converted to OClO. The total number of ClO radicals flown was calculated from the measured ClO concentration flown through the uncoated tube, flow tube length, and contact time. The total amount of OClO produced was determined directly by UV−vis absorption of the gas-phase products evaporating in the sealed, coated flow tube compartment. The results of this set of experiments are shown in Figure 10. Clearly, a nonlinear relation between the number of ClO radicals flown over the ice vs. the number of OClO molecules retrieved from the ice is observed. The solid line represents a quadratic regression analysis of the data points.

We thus believe that the detection of Cl_2O as a minor product in the selfreaction of ClO radicals, as well as the detection of OClO and $ClClO_2$, must be attributed to a heretofore unknown route.

Discussion

Care was taken when preparing the ClO radicals to ensure no unaccounted contaminants were present in the flow, specifically OClO. In typical experimentation, no OClO was detectable in the steady-state flow via UV−vis spectroscopy or TOF MS. Nonetheless, it is conceivable that trace amounts of OClO were generated below the detection limit of the absorption/mass-spectrometric system, and its gradual collection on the ice surface could account for the observed OClO signal upon heating the flow tube. However, this appears to be of only minor importance, since the uptake probability of OClO on ice surfaces was reported by Brown et al.[39] to be insignificant. They had passed OClO over ice at 200 K and noticed no signal decrease as measured with chemical ionization mass spectrometry. Thus, the OClO concentrations observed in the present study cannot result from simple accumulation of OClO present in the flow upon the ice-covered surface.

There are several routes reported in the literature that lead to the different chlorine oxide species observed: Müller and Wilner[27] have described the synthesis of chloryl chloride ($ClClO_2$) through the reaction of $FClO_2$ with BCl_3, or alternatively HCl. Pursell et al.[40] have noted the formation of $ClClO_2$ while studying the photolysis of OClO in polycrystalline ice at 140 K $< T <$ 185 K. They reported that Cl atoms produced by OClO photolysis were able to migrate though the ice cage and react with excess OClO. It is pointed out through this discussion that there exists no experimental evidence that gas-phase reactions of species present in our flow system, in particular ClO radicals, generate Cl_2O or $ClClO_2$. However, several authors have speculated about possible routes for $ClClO_2$ formation in the ClO selfreaction. The formation of $ClClO_2$ in an elementary step is unlikely to occur. McGrath et al.[41] have suggested that isomerization of the unsymmetric dimer ClOClO could lead to indirect formation of chloryl chloride via reactions 11a and b

$$ClO + ClO + M \rightarrow ClOClO + M \qquad (11a)$$

$$ClOClO \rightarrow ClClO_2 \qquad (11b)$$

The possibility that reaction 11a will occur is manifested in the products formed in the bimolecular channel (reaction 6a), OClO, and Cl. Both reactions are exothermic.[42,43] However, Zhu and Lin[42] calculated that isomerization of ClOClO to yield $ClClO_2$ is unlikely to occur due to the high reaction barrier of 79 kJ/mol. Bloss et al.[44] discussed the effect of the possible occurrence of reactions 11a and b on the pressure-dependent formation rate of ClOOCl vs. $ClClO_2$, affecting their absorption cross section measurements at $\lambda = 210$ nm. It is noted that ClOClO is calculated to be far less stable than $ClClO_2$ and ClOOCl.[42,43]

In the present experiments, reactions 11a and b, or other possible routes leading to direct formation of $ClClO_2$ in the gas phase, are considered minor or even negligible. In the absence of ice surfaces, no contributions at the maximum of the $ClClO_2$ absorption ($\lambda = 295$ nm) other than from Cl_2 and ClOOCl were detectable (cf. Figure 4c). In the trap experiment at liquid nitrogen temperatures, very little OClO was recovered (cf. Figure 5). In these runs OClO was present as a reactant, and small amounts entered the cell. Thus, OClO was presumably condensed directly from the gas phase at these low temperatures. As $ClClO_2$ thermally decomposes into Cl_2 and OClO (see below) only very little, if any, contribution from reactions 11a and b are expected to yield chloryl chloride in the absence of ice.

The anhydride of HOCl, Cl_2O, is easily obtained by passing air though an aqueous HOCl solution.[45] Vogt et al.[46] have quantitatively described the temperature effect on the position of the equilibrium (reaction 12, −12) upon flowing the effluent of a 0.1 mol/L aqueous HOCl solution containing an aspirator through a temperature-controlled cold trap. At $T = 200$ K, nearly 25% of the initial HOCl was converted to Cl_2O.

$$2HOCl \rightleftharpoons Cl_2O + H_2O \qquad (12, -12)$$

Based on the observations presented here we postulate that heterogeneous processes occur on/in the ice surface to generate the detected chlorine oxides. Before the discussion of the proposed condensed phase chemistry, the still-unresolved discrepancy with respect to reported ClO reaction probabilities on water/ice surfaces requires discussion. Uptake coefficients ranging between $10^{-5} < \gamma \geq 10^{-2}$ have been measured for ClO. The upper limit is reported by Leu,[47] employing a flow system held at $T = 195$ K with mass spectrometric detection of ClO^+, at an ionization energy of 40 eV. ClO radicals were generated using the Cl + OClO and Cl + Cl_2O reactions. Leu states that an observed production of Cl_2 and O_2 in their flow system is most likely the major product of a surface recombination reaction. The latter speculation is incompatible with our measurements, since we were not able to detect any reaction products when ice was present. In separate experiments it has been shown that Cl_2, once heterogeneously formed on ice surfaces at comparable temperatures, is quantitatively released to the gas phase, for example, in the reaction of HOCl with HCl.[48−50] Martin et al.[51] report a temperature-dependent uptake coefficient of ClO on sulfuric acid/water mixtures that yields $\gamma = (1.1 \pm 0.8) \times 10^{-3}$ at $T = 210$ K. They also measured HCl to be the major reaction product found in the condensed phase, accounting for 80 to 100% of reacted ClO radicals. This latter finding is in accordance with our present results; we have consistently found large amounts of HCl released to the gas phase when evaporating the ice surface. Kenner et al.[52] as well as Abbatt[53] report ClO-uptake coefficients of $\gamma \leq 10^{-4}$ for the interaction with water−ice as well as with 60 and 70 wt. % sulfuric acid. Both studies were conducted in flow tubes employing electron impact mass spectrometry for detection; the temperatures were 183 and 213 K, respectively.

In the present study, the focus was on the products generated in the reaction of ClO radicals with/on ice surfaces rather than on the determination of the respective uptake coefficient. The shortest differential contact time used was approximately 200 ms but frequently on the order of seconds. However, in one set of experiments employing setup C (cf. Figure 2), the ClO flow was exposed to the ice surface for integral contact times ranging from 5 to 60 s and then brought to room temperature. The measured [ClO] in the flow as well as the total amount of OClO recovered are both plotted in Figure 10. Clearly, the efficiency of ClO surface trapping increases with exposure time, that is, with surface loading. Using the gas collision theory equation $Z_{ClO} = A[ClO](RT/2\pi M)^{1/2}$ for the ClO wall collision rate and assuming a 100% conversion of surface-trapped ClO into OClO (see below), an upper limit for the reaction probability of $\gamma_{ClO} = 1 \times 10^{-3}$ can be calculated from the initial slope of the graph and the experimental parameters (flow velocity = 1.5 m/s, [ClO] = $2-5 \times 10^{12}$ molecules/cm^3, and geometrical ice covered surface area = 235 cm^2). This value is not in agreement with the most recent data from Abbatt[53] and Kenner et al.,[52] but agrees well with the measurements from Martin et al.[51] At longer exposure times of the ice surface to ClO radicals γ is calculated to increase to values $>2 \times 10^{-3}$. Further below we will show that our results suggest the value of γ_{ClO} to be strongly dependent on both $[H_2O]_g$ as well as $[ClO]_g$, considering the observation that homogeneous gas-phase ClO recombination reaction to yield the symmetric ClO dimer as a gas-phase reaction product appears to be inhibited in the presence of an ice surface.

Most of the experiments in the present study were carried out at temperatures around $T = 225$ K. The gases entering the ice-covered tube were thus exposed to water concentrations close to the vapor pressure of water on the order of 10^{15} molecules/cm^3 at 225 K. The available literature data on ClO uptake were observed to strongly vary based upon experimental parameters, in particular $[H_2O]_g$, initial $[ClO]_g$, and temperature. Table 1 summarizes the experimental conditions as well as they could be extracted from the reports, with emphasis on the water-vapor concentration. It appears that under conditions of very low $[H_2O]_g$, as in the study of Kenner et al., and/or comparably low initial $[ClO]_g$, as in both studies of Kenner et al.[52] and Abbatt,[53] low γ-values $\leq 10^{-4}$ are observed. With increasing concentrations of either ClO and/or water, as in the study of Martin et al.[51] and the present investigation, significantly higher γ-values of $\approx 10^{-3}$ are observed.

An exception is the study of Leu[47] reporting the highest value of $\gamma > 10^{-2}$. In this study the calculated equilibrium water vapor concentration at $T = 195$ K is only 2.9×10^{13} molecules/cm^{-3}. The paper does not clearly state the initial $[ClO]_g$, however there is more concern about the dynamic source of the radicals in conjunction with mass spectrometric detection, which was carried out at $m/z = 51$ ($^{35}ClO^+$) using 40 eV electron energy. Leu[47] employed the Cl_2O + Cl and OClO + Cl source for radical generation, with the stable compounds being in excess. The appearance potential of ClO^+ from Cl_2O and OClO is 12.5 and 13.5 eV, respectively.[54] It thus appears that the signal at $m/z = 51$ was mostly due to ionic fragmentation of the excess species and to a far lesser extent direct ClO ionization. Identical observations were made in the present study when using mass-spectrometric detection. In fact, at electron energies of 70 eV the fragment signals dominate the mass spectrum, with an abundance of 100% for Cl_2O and 41% for OClO.[55] Small variations due to surface adsorption in the excess components, in particular Cl_2O, would thus result in significant changes in the signal response at $m/z = 51$.

Thus, it appears that an increased availability of gaseous water molecules increases the observed sticking coefficient for ClO. The speculated effect of $[H_2O]_g$ and $[ClO]_g$ on the apparent reactive uptake of ClO radicals toward ice surfaces is further noticeable in the lack of any detectable gas-phase products when running the experiment in the presence of ice. It is conceivable that this most striking difference originates in a "shielding effect" of the reactive site of ClO radicals when water molecules are present. In the formation of the symmetric dimer ClOOCl, this reactive site is the oxygen atom. Francisco and Sander[56] used ab initio calculations to propose the existence of a stable ClO·H_2O-bound complex in the gas phase. In a more recent study Li and Francisco[57] predict the geometry of this complex, using the QCISD method and full optimization up to the 6-311G-(2df, 2p) basis set, to be HOH−OCl with strong hydrogen bonding between one of the H-atoms of water and the ClO oxygen atom. The calculated value of the equilibrium constant for the complex formation is estimated by Francisco and Sander[56] to be $<10^{-19}$ cm^3/molecule, however this as yet has not been determined experimentally. Schindell[58] carried out model studies on ClO·O_2 complexes, focusing on their ability to *enhance* the rate of ClO dimer formation. It was discussed that the excess energy from the reaction of ClO and ClO·O_2 could be imparted to the O_2 as it left the intermediate, and the reaction would no longer require a third body. However, Schindell[58] also reported that calculated dimer formation rates were significantly *decreased* when the postulated ClO·O_2 complex was more stable than assumed. This is in accord with our present results, which show a strong effect on the homo-

TABLE 1: Comparison of Reactive Uptake Coefficients and Experimental Parameters for the Reaction of ClO Radicals on Ice and Sulfuric Acid

[molecule cm^{-3}]					
10^{-12} $[ClO]_g$	10^{-12} $[H_2O]_g$	T [K]	surface type	$10^3\,\gamma$	ref
(no data)	12[a]	190	H_2O ice	>10	Leu[47]
0.2−0.3	4[a]	183	H_2O ice	0.08 ± 0.2	Kenner et al.[52]
0.1−0.2	370[a]	213	H_2O ice 60−70% H_2SO_4	<0.1	Abbatt[53]
∼1000[b]	20[c]	210	60% H_2SO_4	1.2 ± 0.8	Martin et al.[51]
3−8	∼2000[a]	225	H_2O ice	∼1[d]	this work

Note: All entries are rounded. [a] Calculated using the ideal gas law and temperature-dependent equilibrium water vapor pressure above ice. Data from *CRC Handbook of Chemistry and Physics*.[78] [b] Estimate from model calculations as reported in Martin and Wren.[79] [c] Fixed H_2O partial pressure by flowing the carrier gas through a temperature controlled trap filled with H_2O ice. [d] Initial value = lower limit. γ reaches values >0.02 at long exposure times of the ice surface to ClO radicals. Rough estimate only, see Discussion section.

geneous symmetric ClO dimer formation route in the presence of an ice surface and thus also increased water vapor concentrations.

Taking into account the results from the theoretical studies, the speculated dependence of the ClO uptake coefficient on $[H_2O]_g$ and initial [ClO], and the lack of any detectable ClO gas-phase dimerization products in the presence of water at $T = 220$ K, we propose the following primary reaction sequence:

$$ClO(g) + H_2O(g) \rightleftharpoons ClO{\cdot}H_2O(g) \qquad (13, -13)$$

$$ClO{\cdot}H_2O(g) \rightarrow ClO{\cdot}H_2O(s) \qquad (14)$$

Alternatively, upon surface collision, ClO radicals could take up a water molecule:

$$ClO(g) + H_2O(s) \rightarrow ClO{\cdot}H_2O(g) \qquad (15)$$

As an important consequence, $[ClO{\cdot}H_2O(g)]$ would increase with water partial pressure. Based on the data reported by Francisco and Sander,[56] it appears as if the absolute fraction of complexed ClO radicals is too low to effectively inhibit dimer formation. However, one would expect the affinity of the $ClO{\cdot}H_2O$ complex for an ice surface to be much higher than that of free ClO radicals, and in fact would help in increasing the average residence time of ClO radicals on the surface. Thus, a considerable amount of gas-phase ClO would be deposited onto the polar surfaces and rapidly lead to a monolayer of coverage.[59] Using a simple kinetic model assuming $k_{13}/k_{-13} = K = 10^{-19}$ cm^3/molecule[56] and $\gamma(ClO{\cdot}H_2O(g)) = 0.1$, in addition to typical present experimental parameters, $[ClO(g)]_0 = 1 \times 10^{12}$ molecules/cm^3 and $[H_2O(g)] = 1.5 \times 10^{15}$ molecules/cm^3, it is calculated[28] that within 750 ms approximately 50% of the gas-phase ClO radicals present at $t = 0$ are taken up by the surface. These numbers are consistent with our experimental observations reported above.

In a subsequent step, gas-phase ClO reacts with surface-bound ClO, or surface-bound ClO react with each other, in a disproportionation reaction 16a

$$\overset{II}{ClO}(g) + \overset{II}{ClO{\cdot}H_2O}(s) \rightarrow \overset{I}{HOCl}(s) + H^+ + \overset{III}{OClO^-} \qquad (16a)$$

The relatively strong chlorous acid ($K_a = 1.2 \times 10^{-2}$ L/mol)[60] can be expected to ionize quantitatively under the conditions present. Using eq (1)[61] the fraction of dissociated HOClO molecules at concentrations $\leq 10^{-4}$ mol/L is calculated to be > 99%, and ≈65% at concentrations of 10^{-2} Mol/L.

$$\%Diss = -\frac{K_a}{2} \pm \sqrt{\frac{K_a^{\,2}}{4} + K_a[HA]} \cdot \frac{100}{[HA]} \qquad (1)$$

In contrast, the very weak hypochlorous acid ($K_a = 2.3 \times 10^{-8}$ L/mol)[60] is expected to be less than 5% dissociated, even at concentrations $<10^{-5}$ mol/L. Taking the OClO recovery experiments as a basis, as many as 10^{19} molecules ClO were flown over the ice surface. Assuming a 100% conversion rate for the long contact times and 1 mL as the average value for the amount of water deposited on the tube walls, it follows that the average maximum concentration of HOCl and HOClO in the ice layer is on the order of 10^{-2} mol/L. Under these conditions, a fraction of the HOCl will then form the anhydride Cl_2O. Both latter compounds are very likely to be released into the gas phase. Cl_2O has been experimentally observed as a minor product in the REMPI experiments described above. Although no ice surface was prepared in these runs, the in situ OClO generation required moisture to be present in the packed reactor. This water entered the cold flow tube and condensed on the walls. Since the amount of water vapor under such conditions is considerably lower as compared to experiments with an ice surface deliberately prepared, only a small fraction of the ClO radicals could have reacted according to reaction 16a; the majority would react according to reaction 3 and form the symmetric dimer, as shown in Figure 4.

Alternative *homogeneous* pathways for generation of HOCl and HOClO are conceivable. Under the present experimental conditions, that is, an ice surface present and $[H_2O]$ on the order of 10^{15} molecules/cm^3, reactions 16b−d would lead to similar products:

$$ClO{\cdot}H_2O(g) + ClO(g) + nH_2O \rightarrow HOCl(g) + HOClO(g) + nH_2O \qquad (16b)$$

$$HOClO(g) \rightarrow HOClO(s) \qquad (16c)$$

$$HOClO(s) \rightarrow H^+(s) + OClO^-(s) \qquad (16d)$$

[(g) indicates gas, (s) indicates condensed phase, respectively]

Provided the thermal lifetime of HOClO allows for an effective deposition on the ice surface, this reaction sequence appears to be feasible. The relative thermodynamic stabilities, structures, and spectroscopy[62−66] of $HClO_2$ isomers, that is, HOOCl, HOClO, and $HClO_2$, as well as the potential energy surfaces,[67] have been subject to several recent theoretical studies. Depending on the level of theory, the results indicate that the first two structures are considerably more stable than the $HClO_2$ isomer, with HOClO being 10−15 kcal and $HClO_2$ about 55 kcal more endothermic than HOOCl. Furthermore, recent experimental work in Argon matrixes has shown the existence of both former isomers.[68]

Homogeneous reactions of the type depicted by 16b are gaining increasing attention in atmospheric chemistry. A number of high-level ab initio calculations have shown that small numbers of H_2O molecules participating in transition states

dramatically alter the potential energy profile of a reaction. For example, the hydrolysis pathway of SO_3 has a high activation barrier of 32 kcal/mol,[69] and thus is not suggested to lead to the homogeneous formation of H_2SO_4.[70] However, in a theoretical study, Larson et al.[71] have shown that the activation barrier is significantly lowered if a second H_2O molecule participates in the transition state, and even becomes negative for $n = 4$ water molecules:

$$SO_3 \cdot H_2O(g) + nH_2O \rightarrow H_2SO_4(g) + nH_2O \qquad (17)$$

Since we were unable to detect any gas-phase products other than Cl_2O as a minor component, we suspect the fate of the proposed primary products HOCl and $OClO^-$ to be dominated by condensed phase reactions. The following reactions are extracted from the enormous wealth of information on the chemistry of OClO, available in the review article by Gordon.[72] Most of the literature data are obtained from aqueous phase studies. We focus on reactions of chlorine in the oxidation states (0) and (I) with chlorine(III), that is, Cl_2 and HOCl with $OClO^-$, respectively. To exclusively yield the final products Cl^-, ClO_2 and ClO_3^-, Cl_2 and HOCl react rapidly with chlorite ions in acidified or neutral media.[73,74] Taube and Dodgen[74] studied the reactions of isotopically labeled $*Cl_2$ and HO*Cl with $OClO^-$. They found that the labeled *Cl remained distant from the chlorine atoms in the chlorite at all stages of the reaction. Thus, they proposed the existence of an unsymmetrical intermediate of the type $ClClO_2$ or ClOClO, rather than the symmetrical ClOOCl:

$$*Cl_2 + OClO^- \rightarrow *Cl{-}ClO_2 + *Cl^- \qquad (18)$$

$$HO*Cl + OClO^- \rightarrow *Cl{-}ClO_2 + OH^- \qquad (19)$$

It is noted that $Cl{-}ClO_2$ is the mixed anhydride of HOCl and HOClO. In aqueous solutions at room temperature they continue to speculate that $Cl{-}ClO_2$ thermally decomposes into the final products either via reaction 20 or reaction 21:

$$2*Cl{-}ClO_2 \rightarrow *Cl_2 + 2OClO \qquad (20)$$

$$*Cl{-}ClO_2 + H_2O \rightleftharpoons *Cl- + ClO_3^- + 2H^+ \qquad (21)$$

For the *gas phase*, the proposed thermal decomposition step, reaction 20, has been experimentally verified by Müller and Willner.[27] They observed that gas-phase $ClClO_2$ decomposes in second order at a partial pressure of 1 mbar and $T = 298$ K. The elementary steps generating molecular chlorine are either a reaction of the chlorine atom with a second chloryl chloride molecule (reaction 22b), or the recombination reaction 23:

$$Cl{-}ClO_2 \rightarrow Cl + OClO \qquad (22a)$$

$$Cl + Cl{-}ClO_2 \rightarrow Cl_2 + OClO \qquad (22b)$$

$$Cl + Cl + M \rightarrow Cl_2 + M \qquad (23)$$

The net reaction of reaction 22a and b is identical to reaction 20. Product distributions of the reaction sequences 18 + 20 and 19 + 21 are reported to be strongly dependent on pH and initial concentrations.[73] However, qualitatively, reactions 18−22b are in full agreement with our experimental results.

Jia et al.[75] presented a thorough kinetic study of the HOCl + $OClO^-$ system in the liquid phase at room-temperature that yields gas-phase OClO. The experimental conditions in this study held $OClO^-$ in large excess over HOCl. The authors report the oxidation rate of $OClO^-$ by HOCl to be first order in each reactant, in full agreement with our proposed mechanism. They also found strong dependences in the rates of reaction and product yields on pH and buffer concentrations, and proposed a detailed general acid-catalyzed reaction mechanism. Central to their detailed reaction mechanism is the existence of a *linear* asymmetric chlorine oxide intermediate, ClOClO. The net reaction for OClO production is given as

$$HOCl + 2OClO^- + H^+ \rightarrow 2OClO + Cl^- + H_2O \qquad (24)$$

Qualitatively, this mechanism reproduces our experimental findings after the initial reactive uptake of ClO radicals, that is, gas-phase production of OClO (and HCl) upon ice evaporation. However, it does not explain the detection of significant amounts of the *asymmetric* dimer $Cl{-}ClO_2$ as a stable intermediate reaction product, which appeared as a transient species upon ice evaporation. Another significant difference is the experimental condition $[OClO^-] \gg [HOCl]$ in the Jia et al.[75] study. In all our experiments, any chlorine oxide species present on/in the ice surface had to be generated through ClO-radical uptake and subsequent reactions. The anhydride of HOCl was unequivocally detected as a gas-phase product using REMPI MS, but only at very low concentrations. Thus, the major reaction route of HOCl, if generated as the accompanying product of HOClO in reactions 16a or 16b as speculated, must be within the condensed phase, resulting in initial conditions of $[OClO^-] \approx [HOCl]$.

In summary, it is conceivable that under the present conditions, the $OClO^-$ ions generated react with either HOCl or Cl_2, which was always present in varying amounts depending on the ClO source used. The reaction of $OClO^-$ with Cl_2 would yield $Cl{-}ClO_2$ directly. There is evidence that chloryl chloride is stable in the condensed phase, since no OClO release was detected under cold conditions. OClO was only observed at elevated temperatures when the water matrix was evaporating; in most experiments, a transient absorption of $Cl{-}ClO_2$ preceding the OClO absorption was clearly identified (cf. Figure 9). Reaction 18 could also explain the fact that Martin et al.[51] found HCl as a major reaction product in the cold traps used for their experiments. They used the Cl + O_3 system for ClO generation with Cl_2 as the chlorine atom precursor. Due to the generally low dissociation rate of molecular chlorine in microwave discharges, a relatively large excess of Cl_2 is present when using this ClO radical source. We also found HCl to be a reaction product using EI MS. However, we were unable to quantify the amount generated. As pointed out earlier, qualitatively all results reported for the present experiments were reproduced with every ClO radical source described in the Experimental section, that is, also with very low $[Cl_2]$ present. It is thus concluded that (i) the formation of OClO is favorable via both routes, reaction 18 and reaction 19, and (ii) $Cl{-}ClO_2$ is an intermediate of the $OClO^-$ oxidation by either HOCl or Cl_2 as well as the precursor for OClO generation upon ice evaporation.

Atmospheric Implications. The presence of ice surfaces or elevated concentrations of water affects the selfreaction of ClO radicals in three important ways: (1) The overall formation rate of the symmetric dimer, ClOOCl, is significantly lowered. (2) The reactive uptake coefficient of ClO appears to be not only dependent on temperature but also dependent on $[ClO]_g$ and $[H_2O]_g$. (3) The proposed disproportionation reaction 16a and b, and the subsequent thermal or photolytic decomposition of the asymmetric ClO dimer, leads to enhanced OClO formation rates.

As a result, in the presence of an ice surface the ClO reaction system behaves as if the termolecular component (reaction 3)

becomes *less* important, whereas the bimolecular component leading to OClO formation (reaction 6a) is enhanced, as depicted in the following two formal reaction sequences:

Sequence A

$$ClO + ClO + H_2O \rightarrow HOCl + HOClO \quad (25)$$

$$HOCl + HOClO \rightarrow Cl{-}ClO_2 + H_2O \quad (26)$$

$$Cl{-}ClO_2 \rightarrow Cl + OClO \quad (22a)$$

$$\text{Net: } ClO + ClO \rightarrow Cl + OClO \quad (6a)$$

Sequence B

$$ClO + ClO + H_2O \rightarrow HOCl + HOClO \quad (25)$$

$$HOClO + Cl_2 \rightarrow Cl{-}ClO_2 + HCl \quad (27)$$

$$HOCl + HCl \rightarrow Cl_2 + H_2O \quad (28)$$

$$Cl{-}ClO_2 \rightarrow Cl + OClO \quad (22a)$$

$$\text{Net: } ClO + ClO \rightarrow Cl + OClO \quad (6a)$$

(Note: For clarity, chlorous acid is presented in the undissociated form).

We conclude that ClO collisions with ice particles in the stratosphere could result in OClO formation. Martin et al.[51] determined gas−aerosol collision rates for ClO and Cl atoms at various heights in the stratosphere. At 20 km, they calculated a collision frequency of 1.7×10^{-4} collisions s^{-1} for ClO using the expression

$$Z = 1/4(8RT/\pi M)^{1/2}A \quad (2)$$

from collision theory,[76] where A specifies the aerosol surface area per unit volume. If the lower limit for γ_{ClO} of $<10^{-4}$ is applied, reaction rates of ClO and ice particulates on the order of 10^{-8} result, which Martin et al.[51] reported too low to affect the population of species in the stratosphere, specifically chlorine radicals. However, these authors used a stratospheric average for their calculation. In fact, A-values for ice particulates in the polar vortex are different. Using the average ice particulate specific surface area, determined from data taken over McMurdo Station in Antarctica,[77] a ClO−ice particulate collision rate of 3×10^{-3} s^{-1} can be calculated. Applying our observed reaction probability results in a ClO−ice particulate reaction rate $\geq 2.7 \times 10^{-6}$ s^{-1}. Martin et al.[51] reported ClO−ice particulate reaction rates on the order of 10^{-7} high enough to have a significant effect on the population of ClO radicals in the stratosphere. If the $ClO{\cdot}H_2O$ complex indeed exists as predicted by Francisco and Sander,[56] the residence time of this species on ice particulates in the polar vortex, and thus reactivity, would be significantly greater, owing to the elevated accommodation coefficient of the water complex relative to uncomplexed ClO.

In addition to the disagreement in the observed and modeled OClO concentrations, Pierson et al.[15] reported an enhanced [ClO] at 20 km at sunrise in the arctic polar vortex during winter. To model this phenomenon, the magnitude of the OClO concentration was increased in the area where the enhanced ClO density was observed. The authors go on to report that nighttime chemistry not involving BrO was producing a significant amount of OClO, which was enhancing the ClO profile due to OClO photolysis. The reaction of ClO on ice to produce either OClO or its precursor, $ClClO_2$, would occur at night, as it is not dependent on any type of radiation. Also, this reaction occurs regardless of the presence of BrO. Photolysis of both OClO and $ClClO_2$ would result in ClO production:

$$Cl{-}ClO_2 + h\nu \rightarrow Cl + OClO \quad (29)$$

$$Cl + O_3 \rightarrow ClO + O_2 \quad (1)$$

$$OClO + h\nu \rightarrow O + ClO \quad (9)$$

It is thus conceivable that reactions involving the $ClO{\cdot}H_2O$ complex participate in the nighttime chemistry providing the enhanced ClO at sunset, as observed by Pierson et al.[15]

Conclusions

ClO radicals passed over water−ice surfaces were shown to produce significant amounts of several chlorine species, including $Cl{-}ClO_2$ and OClO as major products. It is argued that these chlorine compounds are evolving from a ClO disproportionation reaction occurring on the ice surface, initiated by formation of a $ClO{\cdot}H_2O$ bound complex, proposed by ab initio calculations to exist. This new route of OClO formation has atmospheric implications. First, the BrO + ClO reaction, currently considered the only source of OClO in the stratosphere, is not involved. Several studies have reported the BrO/ClO reaction to be insufficient to describe observed conditions in the stratosphere, and more specifically have shown models of this system to significantly underestimate observed OClO abundances. Second, the rate of the homogeneous recombination of ClO radicals to yield the symmetric ClOOCl dimer is strongly affected by the presence of an ice surface; in this case, production of ClOOCl was not observed. Third, the reactive uptake coefficient of ClO radicals complexed by H_2O is speculated to be significantly larger than the currently accepted value for ClO radicals, strongly depending on $[H_2O]_g$ and $[ClO]_g$.

We believe that the formation of $ClO{\cdot}H_2O$ complexes in the atmosphere can have significant implications on ClO and OClO concentrations. Evidence for the existence of a $ClO{\cdot}H_2O$ complex has yet to be acquired, thus the implications on the total OClO budget cannot be quantitatively determined. However, due to the observed efficiency of the discussed chemistry, it is likely that to some extent the discrepancy between modeled and measured OClO profiles can be accounted for by the heterogeneous source described in this contribution.

Acknowledgment. This work was supported by the BMFT, Bonn, Germany (Grant 01 LO 9520/6 and 07AK 302/0). JRM and MFA acknowledge the receipt of a travel grant and research fellowship from the University of Kiel, Germany. UK acknowledges the receipt of a Promotions Stipendium of the State of Schleswig Holstein, Germany. The authors are obliged to Prof. H. Willner, University of Wuppertal, Germany, for providing the $FClO_2$ and BCl_3 samples as well for his help in the synthesis of $ClClO_2$ and fruitful discussions during the preparation of the present paper.

References and Notes

(1) Molina, M. J.; Rowland, F. S. *Nature* **1974**, *249*, 810.
(2) Geller, M. A.; Yudin, V.; Douglass, A. R.; Waters, J. W.; Elson, L. S.; Roche, A. E.; Russell, J. M., III *Geophys. Res. Lett.* **1995**, *22*, 2937.
(3) Siskind, D. E.; Froidevaux, L.; Russell, J. M.; Lean, J. *Geophys. Res. Lett.* **1998**, *25*, 3513.
(4) Farman, J. C.; Gardiner, B. G.; Shanklin, J. D. *Nature* **1985**, *315*, 207.
(5) Sanders, R. W.; Solomon, S.; Smith, J. P.; Perliski, L.; Miller, H. L.; Mount, G. H.; Keys, J. G.; Schmeltekopf, A. L. *J. Geophys. Res.* **1993**, *98*, 7219.

(6) Hayman, G. D.; Davies, J. M.; Cox, R. A. *Geophys. Res. Lett.* **1986**, *13*, 1347.
(7) Horowitz, A.; Crowley, J. N.; Moortgat, G. K. *J. Phys. Chem.* **1994**, *98*, 11924.
(8) Nickolaisen, S. L.; Friedl, R. R.; Sander, S. P. *J. Phys. Chem.* **1994**, *98*, 155.
(9) Schiller, C.; Wahner, A. *Geophys. Res. Lett.* **1996**, *23*, 1053.
(10) Solomon, S. *Nature* **1990**, *347*, 347.
(11) Wahner, A.; Schiller, C. *J. Geophys. Res.* **1992**, *97*, 8047.
(12) Anderson, J. G.; Toohey, D. W.; Brune, W. H. *Science* **1991**, *251*, 39.
(13) Fish, D. J.; Burton, M. R. *J. Geophys. Res.* **1997**, *102*, 25537.
(14) Miller, H. L., Jr.; Sanders, R. W.; Solomon, S. *J. Geophys. Res.* **1999**, *104*, 18769.
(15) Pierson, J. M.; McKinney, K. A.; Toohey, D. W.; Margitan, J.; Schmidt, U.; Engel, A.; Newman, P. A. *J. Atmos. Chem.* **1999**, *32*, 61.
(16) Woyke, T.; Mueller, R.; Stroh, F.; McKenna, D. S.; Engel, A.; Margitan, J. J.; Rex, M.; Carslaw, K. S. *J. Geophys. Res.* **1999**, *104*, 18755.
(17) Molina, M. J.; Colussi, A. J.; Molina, L. T.; Schindler, R. N.; Tso, T.-L. *Chem. Phys. Lett.* **1990**, *173*, 310.
(18) Kirchner, U.; Liesner, M.; Benter, T.; Schindler, R. N. *Formation of OClO and Cl_2O_3 on Ice in the Cl/O_3−System at Temperatures Below −60 °C and Some Results from the Br/O_3−System*; Presented at STEP−HALOCSIDE/AFEAS Workshop, March 23−25, 1993, Dublin.
(19) Schmidt, S. REMPI Mass Spectrometric Investigations of the Photolysis of Halogen Oxides. Ph.D. Thesis, University of Kiel, 1997.
(20) Kirchner, U. Laboratory Studies of Atmospherically Relevant Heterogeneous Reactions of Halogen Oxides. Ph.D. Thesis, University of Kiel, 1997.
(21) Garnica, R. M.; Appel, M. F.; Eagan, L.; McKeachie, J. R.; Benter, T. *Anal. Chem.* **2000**, *72*, 5639.
(22) Benter, T.; Liesner, M.; Sauerland, V.; Schindler, R. N. *Fresenius' J. Anal. Chem.* **1995**, *351*, 489.
(23) Schmidt, S.; Appel, M. F.; Garnica, R. M.; Schindler, R. N.; Benter, T. *Anal. Chem.* **1999**, *71*, 3721.
(24) Bleaching Agents. In *Kirk-Othmer Encyclopedia of Chemical Technology*, 2nd ed.; Wiley & Sons: New York, 1964; Vol. 3, p 550.
(25) Renard, J. J.; Bolker, H. I. *Chem. Rev.* **1976**, *76*, 487.
(26) Cady, G. H. Chlorine (I) Compounds. In *Inorganic Syntheses*; Moeller, T., Ed.; McGraw-Hill: New York, 1957; p 156.
(27) Müller, H. S. P.; Willner, H. *Ber. Bunsen-Ges. Phys. Chem.* **1992**, *96*, 427.
(28) Deuflhard, P.; Bader, G.; Nowak, U. LARKIN—A Software Package for the Numerical Simulation of LARge Systems Arising in Chemical Reaction KINetics. In *Springer Series Chem. Phys.*; Ebert, K. H., Deuflhard, P., Jäger, W., Eds.; Springer-Verlag: Berlin, 1981; Vol. 18, p 38.
(29) DeMore, W. B.; Howard, C. J.; Sander, S. P.; Ravishankara, A. R.; Golden, D. M.; Kolb, C. E.; Hampson, R. F.; Molina, M. J.; Kurylo, M. J. *Chemical Kinetics and Photochemical Data for Use in Stratospheric Modeling, Evaluation No. 12, JPL Publication No. 97-4; JPL Publication No. 97-4 ed.*; Jet Propulsion Laboratory, California Institute of Technology: Pasadena, CA, 1997.
(30) Robin, M. B. Multiphoton Spectroscopy and Photochemistry. In *Advances in Laser Spectroscopy*; Garetz, B. A., Lombardi, J. R., Eds.; John Wiley & Sons: New York, 1986; Vol. 3, p 147.
(31) Schmidt, S.; Benter, T.; Schindler, R. N. *Chem. Phys. Lett.* **1998**, *282*, 292.
(32) Cooper, M. J.; Diez-Rojo, T.; Rogers, L. J.; Western, C. M.; Ashfold, M. N. R.; Hudgens, J. W. *Chem. Phys. Lett.* **1997**, *272*, 232.
(33) Coxon, J. A. *Can. J. Phys.* **1979**, *57*, 1538.
(34) Liesner. REMPI Mass Spectrometric Investigations of ClO-Containing Compounds. Ph.D. Thesis, University of Kiel, 1995.
(35) Takahashi, K.; Wada, R.; Matsumi, Y.; Kawasaki, M. *J. Phys. Chem.* **1996**, *100*, 10145.
(36) Baumgärtel, S.; Gericke, K.-H. *Chem. Phys. Lett.* **1994**, *227*, 461.
(37) Thorn, R. P., Jr.; Stief, L. J.; Kuo, S.-C.; Klemm, R. B. *J. Phys. Chem.* **1996**, *100*, 14178.
(38) De Haan, D. O.; Birks, J. W. *J. Phys. Chem.* **1997**, *101*, 8026.
(39) Brown, L. A.; Vaida, V.; Hanson, D. R.; Graham, J. D.; Roberts, J. T. *J. Phys. Chem.* **1996**, *100*, 3121.
(40) Pursell, C. J.; Conyers, J.; Denison, C. *J. Phys. Chem.* **1996**, *100*, 15450.
(41) McGrath, M. P.; Clemitshaw, K. C.; Rowland, F. S.; Hehre, W. J. *J. Phys. Chem.* **1990**, *94*, 6126.
(42) Zhu, R. S.; Lin, M. C. *J. Chem. Phys.* **2003**, *118*, 4094.
(43) Lee, T. J.; Rohlfing, C. M.; Rice, J. E. *J. Chem. Phys.* **1992**, *97*, 6593.
(44) Bloss, W. J.; Nickolaisen, S. L.; Salawitch, R. J.; Friedl, R. R.; Sander, S. P. *J. Phys. Chem.* **2001**, *105*, 11226.
(45) Downs, A. J.; Adams, C. J. *Comprehensive Inorg. Chem.* **1973**, *2*, 1361
(46) Vogt, R.; Schindler, R. N. *Ber. Bunsen-Ges. Phys. Chem.* **1993**, *97*, 819.
(47) Leu, M.-T. *Geophys. Res. Lett.* **1988**, *15*, 851.
(48) Caldwell, T. E.; Foster, K. L.; Benter, T.; Langer, S.; Hemminger, J. C.; Finlayson-Pitts, B. J. *J. Phys. Chem.* **1999**, *103*, 8231.
(49) Foster, K. L.; Caldwell, T. E.; Benter, T.; Langer, S.; Hemminger, J. C.; Finlayson-Pitts, B. J. *PCCP* **1999**, *1*, 5615.
(50) Kirchner, U.; Benter, T.; Schindler, R. N. "Some Low-Temperature Heterogeneous Reactions of the Type ROX + HCl → XCl + ROH (R = CH_3, H; X = Cl, Br) on Doped Ice", submitted for publication.
(51) Martin, L. R.; Judeikis, H. S.; Wun, M. *J. Geophys. Res.* **1980**, *85*, 5511
(52) Kenner, R. D.; Plumb, I. C.; Ryan, K. R. *Geophys. Res. Lett.* **1993**, *20*, 193.
(53) Abbatt, J. P. D. *Geophys. Res. Lett.* **1996**, *23*, 1681.
(54) *Energetics of Gaseous Ions*; J. Phys. Chem. Ref. Data; Rosenstock, H. M., Draxl, K., Steiner, B. W., Herron, J. T., Eds.; ACS and American Institute of Physics: Washington, DC, 1977; Vol. 6. Supplement No. 1 ed.
(55) NIST Chemistry Webbook, IR and Mass Spectra. In *NIST Standard Reference Database No. 69*.
(56) Francisco, J. S.; Sander, S. P. *J. Am. Chem. Soc.* **1995**, *117*, 9917.
(57) Li, Y. M.; Francisco, J. S. *J. Chem. Phys.* **2001**, *115*, 8381.
(58) Schindell, D. T. *J. Atmos. Chem.* **1997**, *26*, 323.
(59) Sander, S. P.; Friedl, R. R.; DeMore, W. B.; Golden, D. M.; Kurylo, M. J.; Hampson, R. F.; Huie, R. E.; Moortgat, G. K.; Ravishankara, A. R.; Kolb, C. E.; Molina, M. J. *Chemical Kinetics and Photochemical Data for Use in Stratospheric Modeling: Supplement to Evaluation No. 12, JPL Publication No. 00-3; JPL Publcation 00−3 ed.*; Jet Propulsion Laboratory, California Institute of Technology: Pasadena, CA, 2000.
(60) Perrin, D. D. *Dissociation Constants of Inorganic Acids and Bases in Aqueous Solution*; Page Brothers, Ltd: Norwich, 1969.
(61) Zumdahl, S. S.; Zumdahl, S. A. *Chemistry*, 5th ed.; Houghton Mifflin Co.: New York, 2000.
(62) Francisco, J. S.; Sander, S. P.; Lee, T. J.; Rendell, A. P. *J. Phys. Chem.* **1994**, *98*, 5644.
(63) Turner, A. G.; Oleksik, J. *Inorg. Chim. Acta* **1991**, *180*, 15.
(64) Lee, T. J.; Rendell, A. P. *J. Phys. Chem.* **1993**, *97*, 6999.
(65) Mcgrath, M. P.; Clemitshaw, K. C.; Rowland, F. S.; Hehre, W. J. *J. Phys. Chem.* **1990**, *94*, 6126.
(66) Lee, T. J.; Parthiban, S.; Head-Gordon, M. *Spectrochim. Acta, Part A* **1999**, *55*, 561.
(67) Sumathi, R.; Peyerimhoff, S. D. *J. Phys. Chem.* **1999**, *103*, 7515.
(68) Johnsson, K.; Engdahl, A.; Nelander, B. *J. Phys. Chem.* **1996**, *100*, 3923.
(69) Morokuma, K.; Muguruma, C. *J. Am. Chem. Soc.* **1994**, *116*, 10316.
(70) Kolb, C. E.; Jayne, J. T.; Worsnop, D. R.; Molina, M. J.; Meads, R. F.; Viggiano, A. A. *J. Am. Chem. Soc.* **1994**, *116*, 10314.
(71) Larson, L. J.; Kuno, M.; Tao, F. M. *J. Chem. Phys.* **2000**, *112*, 8830.
(72) Gordon, G.; Kieffer, R. G.; Rosenblatt, D. H. *Prog. Inorg. Chem.* **1972**, *15*, 201
(73) Emmenegger, F.; Gordon, G. *Inorg. Chem.* **1967**, *6*, 633.
(74) Taube, H.; Dodgen, H. *J. Am. Chem. Soc.* **1949**, *71*, 3330.
(75) Jia, Z.; Margerum, D. W.; Francisco, J. S. *Inorg. Chem.* **2000**, *39*, 2614.
(76) Present, R. D. *Kinetic Theory of Gases*; McGraw-Hill: New York, 1958.
(77) Adriani, A.; Deshler, T.; Di Donfrancesco, G.; Gobbi, G. P. *J. Geophys. Res.* **1995**, *100*, 25877.
(78) *CRC Handbook of Chemistry and Physics*, 63rd ed.; Weast, R. C., Astle, M. J., Eds.; CRC Press: Boca Raton, Florida, 1984.
(79) Martin, L. R.; Wren, A. G. *Int. J. Chem. Kinet.* **1979**, *11*, 543.
(80) Wayne, R. P.; Poulet, G.; Biggs, P.; Burrows, J. P.; Cox, R. A.; Crutzen, P. J.; Hayman, G. D.; Jenkin, M. E.; Lebras, G.; Moortgat, G. K.; Platt, U.; Schindler, R. N. *Atmos. Environ.* **1995**, *29*, 2677.